

Fairness-aware Vision Transformer via Debiased Self-Attention

Yao Qiang Chengyin Li Prashant Khanduri Dongxiao Zhu
 Department of Computer Science, Wayne State University
 {yao, cyli, khanduri.prashant, dzhu}@wayne.edu

Abstract

Vision Transformer (ViT) has recently gained significant attention in solving computer vision (CV) problems due to its capability of extracting informative features and modeling long-range dependencies through the self-attention mechanism. Whereas recent works have explored the trustworthiness of ViT, including its robustness and explainability, the issue of fairness has not yet been adequately addressed. We establish that the existing fairness-aware algorithms designed for CNNs do not perform well on ViT, which highlights the need for developing our novel framework via Debiased Self-Attention (DSA). DSA is a fairness-through-blindness approach that enforces ViT to eliminate spurious features correlated with the sensitive label for bias mitigation and simultaneously retain real features for target prediction. Notably, DSA leverages adversarial examples to locate and mask the spurious features in the input image patches with an additional attention weights alignment regularizer in the training objective to encourage learning real features for target prediction. Importantly, our DSA framework leads to improved fairness guarantees over prior works on multiple prediction tasks without compromising target prediction performance.

1. Introduction

Recently, Vision Transformer (ViT) [11, 30] has emerged as an architectural paradigm and a viable alternative to the standard Convolutional Neural Network (CNN) [19, 42, 27] in the computer vision (CV) community. ViT is able of extracting global relationships via the self-attention mechanism leading to impressive feature representation capabilities, which has resulted in improved performance in various CV tasks, such as image classification [11, 30], object detection [3, 9], semantic segmentation [67, 55], and image generation [21], to name a few.

Given its promising performance, researchers have studied the trustworthiness of ViT for real-world applications. Several works have explored the robustness and explainability of ViT, highlighting its strengths and weaknesses.

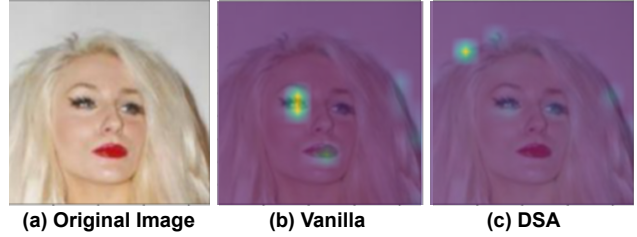


Figure 1: An illustration example. The prediction target label is *Hair Color* and the sensitive label is *Gender*. The heatmap of attention weights shows that the Vanilla ViT uses spurious features, e.g., ‘red lip’ and ‘eye shadow’, whereas the fairness-aware ViT via our DSA leverages the real features, e.g., ‘hair’, for target prediction.

Robustness refers to the ability of ViT to perform well on inputs that deviate from the training distribution, such as adversarial examples [2, 13, 50, 38, 68]. Explainability refers to the ability of ViT to provide insights into its decision-making process, which is crucial for building trust in the model [1, 4, 47].

Besides robustness and explainability, fairness stands as another core trustworthy desiderata [20, 7]. Several studies have already demonstrated that many deep-learning-based models simply make predictions by exploiting spurious correlations with the input features [58, 23]. These spurious correlations occur when a feature is statistically informative for a majority of training examples but does not actually capture the underlying relationship between the input features and the target labels [61, 54].

As the example shown in Figure 1, spurious features like ‘eye shadow’ or ‘red lips’ are spuriously correlated with hair color, but they do not actually capture the underlying relationship between hair color and the other features. Thus, the vanilla ViT simply learns these spurious features as a shortcut to predict the hair color, rather than learning the real features that are actually relevant to the target label as shown in Figure 1(b). This is where the fairness-aware ViT comes in - it is designed to learn real features that are not correlated with the sensitive label, in this case, gender, in

order to make unbiased predictions as shown in Figure 1(c).

Although an array of debiasing algorithms have been proposed [36, 65, 66, 23, 60, 46] for CV tasks, most are designed for learning with the CNN models. Whether these algorithms are compatible or even transferable to the ViT architecture is still an open research question. Regardless of the neural network architecture, limiting the spurious correlation between the input features and the target labels for bias mitigation is still a challenging problem. One key challenge arises from the fact that automatically locating the spurious features in the input images is computationally intractable. For example, one simple solution is to have domain experts and/or crowd workers curate the entire training set, which neither works well with unknown bias [29] nor is scalable to large-scale datasets [39]. Moreover, even if one can identify the spurious features, another major challenge is how to make the classifier blind to such features. Regarding image in-painting [59, 35] as a potential solution, it is worth noting that this approach has some limitations. The success of image in-painting depends heavily on the quality of the in-painting algorithm and the effectiveness of the feature selection process. Additionally, it may be challenging to determine which features to remove and which to keep to preserve image integrity while mitigating bias.

To address the above challenges, we propose a novel framework for ensuring bias mitigation training of ViT via Debiasing Self-Attention (DSA) to decouple the target prediction from the spurious features. DSA takes a hierarchical approach, where the first stage aims to localize and perturb the spurious features from input image patches by leveraging adversarial attacks against a bias-only model. The bias-only model, which is trained with an adversarial learning objective [65], is able to explicitly predict sensitive labels, such as gender and race, by exploiting spurious features maximally while minimally leveraging other features including the real features, such as hair.

DSA relies on the intuitive hypothesis that adversarial attacks, although initially designed to evaluate the robustness of ViT, can also be used to identify and remove spurious features to train debiased ViTs. While the transferability of adversarial attack approaches from CNN to ViT is still a matter of contention in the literature [41, 53, 44, 45, 17], recent work [13] proposes Patch-Fool as a viable approach to attack the self-attention mechanism by targeting image patches during ViT’s self-attention computations. This motivates us to design a novel adversarial attack against the bias-only model with the goal of capturing the most important patches for learning the sensitive label. Different from image in-painting approaches, adversarial examples are automatically constructed during the attack by directly perturbing the patches with spurious features.

In the second stage of DSA, the original training set is augmented with the constructed adversarial examples to

formulate a debiased training set. In addition, a regularizer, which is specifically designed for the self-attention mechanism in ViT, is introduced to align the biased examples and their corresponding unbiased adversarial examples through attention weights. Our novel training objective encourages ViT models to learn informative features while ensuring their fairness.

We summarize our major contributions: (1) We design a novel DSA framework for ViT to mitigate bias in both the training set and learning algorithm via identifying spurious features and retaining real features for target prediction. (2) We tackle several challenges for the under-addressed fairness problem in ViT from a novel perspective of leveraging adversarial examples to eliminate spurious features while utilizing attention weights alignment to retain informative features. (3) Our DSA framework provides a flexible and modular debiasing approach that can be used either on its own or with other fairness-aware training algorithms to ensure ViT fairness. (4) The quantitative experimental results demonstrate that DSA improves group fairness with respect to demographic parity and equality of odds metrics while maintaining competitive or even better prediction accuracy compared to baselines. Our qualitative analysis further indicates that DSA has reduced attention to spurious features, which is a desirable property for bias mitigation.

2. Related Work

ViT for Image Classification. ViT has been a topic of active research since its introduction, and various approaches have been proposed to improve its performance and applicability. The earlier exploration of ViT either used a hybrid architecture combining convolution and self-attention [3] or a pure self-attention architecture without convolution [48]. The work in [11] proposed a ViT that achieves impressive results on image classification using ImageNet data set. This success has motivated a series of subsequent works to further exploit ViT’s expressive power from various perspectives, such as incorporating locality into ViT [28, 30, 63], and finding well-performing ViT using neural architecture search (NAS) [6].

Fairness and Debiased Learning. The field of fairness in deep learning has grown significantly over the past several years as a result of bias in training data and algorithms [36, 46]. The existing techniques for debiased learning can be roughly categorized into pre-, in-, and post-processing.

– **Pre-processing** methods attempt to debias and increase the quality of the training set with the assumption that fair training sets would result in fair models [66, 25, 8]. The work in [66] proposed to balance the data distribution over different protected attributes by generating adversarial examples to supplement the training dataset. Similarly, [25]

generated the bias-swapped image augmentations to balance protected attributes, which would remove the spurious correlation between the target label and protected attributes. In [8], the authors presented fair mixup as a new data augmentation method to generate interpolated samples to find middle-ground representation for different protected groups. The work [46] described a novel generative data augmentation approach to create counterfactual samples that d-separates the spurious features and the targets ensuring fairness and attribution-based explainability.

– **In-processing** approaches aim to mitigate bias during the training process by directly modifying the learning algorithm and model weights with specifically designed fairness penalties/constraints or adversarial mechanism [36, 65, 49, 24, 40]. To enforce the fairness constraints, one line of works either disentangles the association between model predictions and the spurious features via an auxiliary regularization term [40] or minimizes the performance difference between protected groups with a novel objective function [49]. However, the issue is that the trained models may behave differently at the inference stage even though such fairness constraints are satisfied during the training. Another line of works [36, 65, 24, 60] enforce the model to generate fair outputs with adversarial training techniques through the min-max objective: maximizing accuracy while minimizing the ability of a discriminator to predict the protected (sensitive) attribute. Nevertheless, this process can compromise the model performance on the main prediction task. Additional lines of works impose either orthogonality [51], disentanglement [32], or feature alignment [23] constraints on the feature representation and force the representation to be agnostic to the sensitive label. We note that most of these approaches are exclusively designed for CNN architectures, and whether these approaches are transferable to the ViT has not yet been demonstrated.

– **Post-processing** techniques directly calibrate or modify the classifier’s decisions to certain fairness criteria at inference time [26, 33]. These methods require access to the sensitive attribute for fair inference, which may not be feasible in real-world applications due to salient security and privacy concerns.

Fairness in ViT. Recently, [16] explored how the spurious correlations are manifested in ViT and performed extensive experiments to understand the role of the self-attention mechanism in debiased learning of ViT. Despite the new insights, the authors did not provide any debiasing techniques for ViT. The authors in [56] proposed a new method, named TADeT, for debiasing ViT that aims to discover and remove bias primarily from query matrix features. To our knowledge, this is the only published work along the line of fairness ViT. Nevertheless, this pioneering work TADeT has two weaknesses: first, it requires parameter sharing across

the key and value weights in the self-attention mechanism, which may conflict with most ViT architectures; second, the complex alignment strategy on the query matrix is not straightforward, and well investigated. Thus, TADeT does not even outperform the compared baselines that are primarily designed for CNNs.

In contrast to the above works, this work tackles the debiasing problem through a novel perspective of fairness-through-adversarial-attack. The proposed DSA framework combines the strengths of both pre- and in-processing approaches via leveraging data augmentation (for ensuring fairness in the training set) and feature alignment for bias mitigation. The adversarial examples are used to both disentangle spurious features from informative features and to align attention weights, specifically, tailor-made for the self-attention mechanism in ViT. Notably, our approach for the fair ViTs is a novel addition to the growing body of work on “adversarial examples for fairness” [66, 62].

3. Preliminaries

3.1. Overview of Vision Transformer

Similar to the Transformer architecture [57], the ViT model expects the input to be a linear sequence of token/patch embeddings. An input image is first partitioned into non-overlapping fixed-size square patches resulting in a sequence of flattened 2D patches. These patches are then mapped to constant-size embeddings using a trainable linear projection. Next, position embeddings are added to the patch embeddings to imbibe relative positional information of the patches. Finally, the ViT model prepends a learnable embedding (class token) to the sequence of embedded patches following [10], which is used as image representation at the model’s output.

To summarize, the ViT model consists of multiple stacked encoder blocks, where each block consists of a Multi-head Self Attention (MSA) layer and a Feed-Forward Network (FFN) layer. The MSA performs self-attention over input patches to learn relationships between each pair of patches, while the FFN layer processes each output from the MSA layer individually using two linear layers with a GeLU activation function. Both MSA and FFN layers are connected by residual connections.

3.2. Fairness Metrics

Many different notions of fairness have been proposed in the literature [12, 18]. In this work, we mainly focus on the two most widely used definitions: demographic parity [12] and equalized odds [18] as the metrics to assess group fairness of the model. Demographic Parity (DP) measures whether the true positive rates across all groups (defined by a sensitive label s , e.g., gender) are equal, particularly between the vulnerable minority group ($s = 0$) and

others ($s = 1$), formally: $DP = TPR_{s=1} - TPR_{s=0}$. Equalized Odds (EO) is used to understand the disparities in both the true positive rates and the false positive rates in the vulnerable group compared to others: $EO = \frac{1}{2}[TPR_{s=1} - TPR_{s=0}] + \frac{1}{2}[FPR_{s=1} - FPR_{s=0}]$. In addition, we also use Accuracy (ACC) and Balanced Accuracy (BA) [43], where $BA = \frac{1}{4}[TPR_{s=0} + TNR_{s=0} + TPR_{s=1} + TNR_{s=1}]$, to evaluate the utility of the model. However, when a dataset is class imbalanced, BA will have an implicit bias against the minority class. Therefore, we introduce Difference of Balanced Accuracy (DBA) as a way to measure the difference in a model's performance across groups defined by a sensitive label while accounting for class imbalance, formally: $DBA = \frac{1}{2}[TPR_{s=1} + TNR_{s=1}] - \frac{1}{2}[TPR_{s=0} + TNR_{s=0}]$.

3.3. Problem Formulation

We consider a supervised classification task with training samples $\{x, y, s\} \sim p_{data}$, where $x \in \mathcal{X}$ is the input feature, $y \in \mathcal{Y}$ is the target label, and $s \in \mathcal{S}$ is a sensitive label. Some examples of \mathcal{S} include gender, race, age, or other attributes that can identify a certain protected group. We assume that the sensitive label s can only be used during the training phase, and are not accessible during the inference phase. Moreover, we assume that each input feature x can be split into two components, one with *spurious features* \mathbf{x}_s that are highly correlated with the sensitive label s , and the rest \mathbf{x}_t that are *real features* correlated with the target label y , i.e., $\mathbf{x} = (\mathbf{x}_s, \mathbf{x}_t)$.

Deep learning models, including ViT, are trained using a large amounts of data and learn patterns from the data in order to make predictions. However, if the training data is imbalanced or biased, the model can learn spurious patterns that reflect the biases in the data rather than the real patterns. This is a particular problem when there are spurious features \mathbf{x}_s in the data that are highly correlated with the target label y . For example, if a dataset includes information about the race or gender of individuals, and these sensitive labels are highly correlated with certain outcomes, a model trained on that data may learn to use those spurious features to make predictions, a.k.a shortcut learning [15].

This motivates the proposal of our two-step hierarchical DSA framework for bias mitigation. In the first step, DSA localizes and masks the spurious features \mathbf{x}_s from the input x in order to disentangle \mathbf{x}_s from \mathbf{x}_t . This is accomplished by transforming the model prediction from $p(x) = p(y|\mathbf{x}_s, \mathbf{x}_t)$ to $p(x) \propto p(x') = p(y|\mathbf{x}_t')$, where x' is the sample constructed after masking the spurious features \mathbf{x}_s from x via adversarial attacks. In the second step, DSA utilizes the original x and the augmented data x' to train a ViT model $f(\cdot)$, while at the same time satisfying certain fairness requirements (i.e., DP, EO, and DBA) with respect to the sensitive label s .

4. Debaised Self-Attention (DSA) Framework

Our major motivation is to achieve fairness of ViT by mitigating the influence of spurious features (e.g., 'red lip' and 'eye shadow') on the prediction task (*Hair Color*). However, unlike CNN, it is a challenging task to locate the spurious features from the input directly under the ViT framework. To address this challenge, we propose a hierarchical framework as discussed in Section 3.3. Specifically, our DSA framework follows a two-step procedure as shown in Figure 2:

Step 1: a *bias-only* model is trained deliberately to *maximize* the usage of spurious features while *minimize* the usage of the real features for sensitive label prediction. Then, the adversarial examples, in which the spurious features are perturbed, are constructed via adversarial attacks against the *bias-only* model.

Step 2: a *debaised* model is trained with augmented adversarial examples and attention weights alignment aiming to mitigate the influence of spurious features on the prediction task to preserve the accuracy.

4.1. Training the Bias-only Model

Recall that the input features consist of two components $\mathbf{x} = (\mathbf{x}_s, \mathbf{x}_t)$, where \mathbf{x}_s and \mathbf{x}_t denote the spurious and real features, respectively. Our goal is to build the bias-only model which only learns \mathbf{x}_s but neglects \mathbf{x}_t from the input features. The input image x is first fed into the feature extractor of ViT $h: \mathcal{X} \rightarrow \mathbb{R}^k$, where k is the feature dimension. Subsequently, the extracted features $h(x)$ are fed forward through both the sensitive label prediction head $f_s: \mathbb{R}^k \rightarrow \mathcal{S}$ and the target label prediction head $f_t: \mathbb{R}^k \rightarrow \mathcal{Y}$. f_s is trained to minimize the following Cross-Entropy (CE) loss:

$$\mathcal{L}_S(x, s) = \mathcal{L}_{CE}(f_s(h(x), s). \quad (1)$$

And the objective of training f_t is to maximize:

$$\mathcal{L}_T(x, y) = \mathcal{L}_{CE}(f_t(h(x), y). \quad (2)$$

The two prediction heads f_s and f_t of the bias-only model f_B are jointly trained in an adversarial training strategy as:

$$\mathcal{L}_B(x, s, y) = \mathcal{L}_S(x, s) - \mathcal{L}_T(x, y). \quad (3)$$

With this objective, f_s is trained to minimize the CE loss to correctly predict s . While f_t is trained to maximize the CE loss to refrain f_t from predicting y .

In practice, h , f_t , and f_s in the bias-only model f_B are trained jointly with both adversarial strategy [65] and gradient reversal technique [14]. Early in the learning, $f_s \odot h$ is rapidly trained to predict s using spurious features. Then f_t learns to refrain from predicting y , and h learns to extract spurious features that are independent of y . At the end of

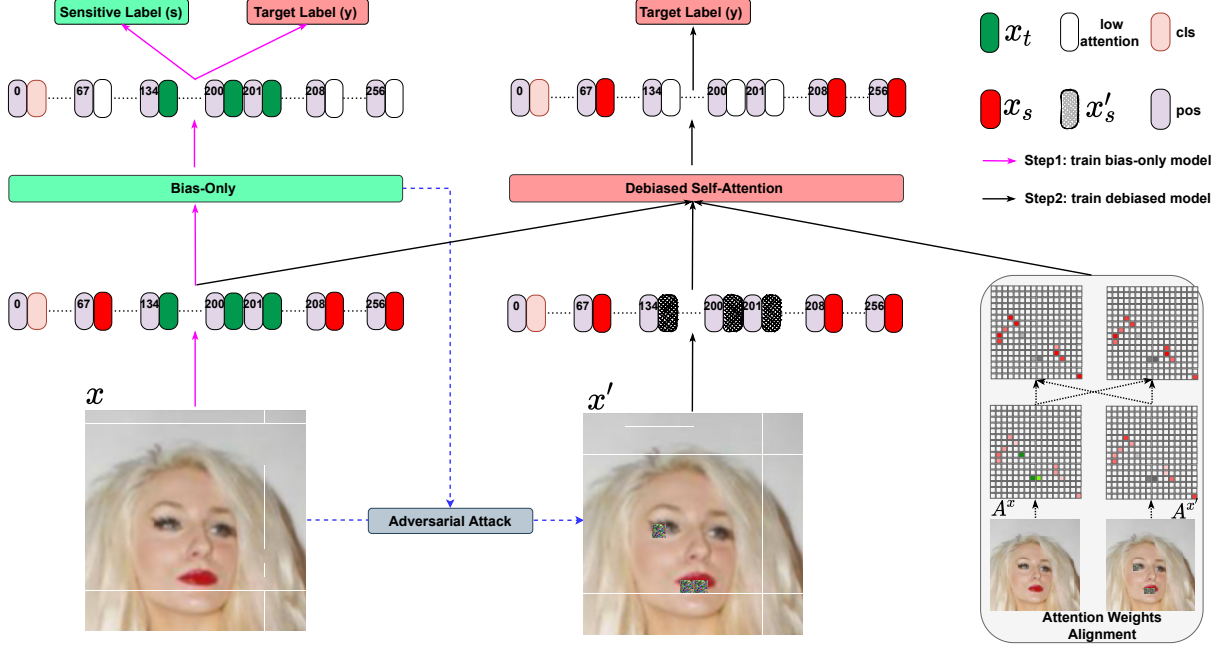


Figure 2: The DSA framework. The prediction target label is *Hair Color* and the sensitive label is *Gender*. The bias-only model is first trained to learn the *spurious features* (the green patches) for predicting sensitive label s but not to learn the real features (the red patches) with an adversarial objective (see Section 4.1). The adversarial attack is then applied against the bias-only model to generate the adversarial examples x' , by perturbing the spurious features (the grid shadow patches) of the original inputs x (see Section 4.2). Finally, both x and x' are used to train a fairness-aware ViT with an attention weights alignment objective (see Eq. (13)) and learn the *real features* (the red patches) (see Sections 4.3 and 4.4).

the training, f_B performs poorly in predicting the target label y yet performs well in predicting the sensitive label s . It is not due to the divergence but due to the feature extractor h **unlearns** the real features. As such, $h(x)$ extracts largely spurious features instead of real features for the subsequent debiasing of ViT in Step 2.

We illustrate this idea using the example in the left panel of Figure 2. We consider the *Hair Color* prediction task with *Gender* bias. The bias-only model f_B mainly relies on the spurious features, like ‘eye shadow’ and/or ‘red lips’, to predict the sensitive label s (e.g., *Gender*), while at the same time paying nearly no attention to the real features, i.e., ‘hair’, to predict the target label y (e.g., *Hair Color*).

4.2. Adversarial Attack Against the Bias-only Model

After building the bias-only model f_B , DSA uses adversarial attacks to construct augmented adversarial examples in which the spurious features are localized and perturbed as shown in Figure 2. Since ViTs and CNNs have different architectures and input formats, traditional adversarial attacks, which are originally designed for CNNs, are not effective against ViTs [13]. Inspired by the idea of Patch-Fool [13], we design a novel adversarial attack method aiming to

localize and perturb the spurious features in the inputs and retain the real features at the same time. Specifically, our attack method is designed to compromise the self-attention mechanism in the pre-trained bias-only model by attacking its basic component (i.e., a single patch) with a series of attention-aware optimization techniques. In more details, given $\mathcal{L}_S(x, s)$, $\mathcal{L}_T(x, y)$, and a sequence of input image patches $\mathbf{X} = [\mathbf{x}_1, \dots, \mathbf{x}_p, \dots, \mathbf{x}_n]^T \in \mathbb{R}^{n \times d}$ with its associated sensitive label s , and target label y , the objective of the adversarial attack algorithm is

$$\arg \max_{1 \leq p \leq n, \mathbf{E} \in \mathbb{R}^{n \times d}} \mathcal{L}_S(\mathbf{X} + \mathbf{1} \odot \mathbf{E}, s) \quad (4)$$

$$+ \arg \min_{1 \leq p \leq n, \mathbf{E} \in \mathbb{R}^{n \times d}} \mathcal{L}_T(\mathbf{X} + \mathbf{1} \odot \mathbf{E}, y), \quad (5)$$

where \mathbf{E} denotes the adversarial perturbation; $\mathbf{1} \in \mathbb{R}^n$ is the identifying one-hot vector demonstrating whether current p -th patch is selected or not; \odot represents the penetrating face product [13].

This adversarial attack algorithm proceeds by (1) select the adversarial patch p , and (2) optimize the corresponding adversarial attack, \mathbf{E} .

Selection of p : For encoder blocks in the ViT, we define: $t_j^{(l)} = \sum_{h,i} a_j^{(l,h,i)}$ to measure the importance of the j -th patch in the l -th block based on its contributions to other

patches in the self-attention calculation, where $\mathbf{a}^{(l,h,i)} = [a_1^{(l,h,i)}, \dots, a_n^{(l,h,i)}]$ denotes the attention distribution for the i^{th} patch of the h^{th} head in the l^{th} block. Our motivation is to localize the most influential patch p according to the predicted sensitive label s but with the least impact on predicting target label y . Here, we derive the top k (which is a tunable hyper-parameter) important patches from $\arg \max t_j^{(l)}$.

Optimize E: Given the selected adversarial patch index p from the previous step, an attention-aware loss is applied for the l^{th} block as $\mathcal{L}_{\text{Attn}} = \sum_{h,i} a_p^{(l,h,i)}$. This loss is expected to be maximized so that the adversarial patch p , serving as the target adversarial patch, can attract more attention from other patches for effectively fooling ViTs. The perturbation \mathbf{E} is then updated based on both the final sensitive label classification loss and a layer-wise attention-aware loss:

$$\mathcal{L}(\mathbf{X}', s, p) = \mathcal{L}_S(\mathbf{X}', s) - \mathcal{L}_T(\mathbf{X}', y) \quad (6)$$

$$+ \alpha \sum_l \mathcal{L}_{\text{Attn}}(\mathbf{X}', p), \quad (7)$$

where $\mathbf{X}' \triangleq \mathbf{X} + \mathbf{1} \odot \mathbf{E}$ and α is a weight hyper-parameter set to 0.5 in the experiments. Moreover, PCGrad [64] is adopted to avoid the gradient conflict of the two losses and \mathbf{E} is updated using:

$$\delta_{\mathbf{E}} = \nabla_{\mathbf{E}} \mathcal{L}(\mathbf{X}', s, p) - \alpha \sum_l \beta_l \nabla_{\mathbf{E}} \mathcal{L}_S(\mathbf{X}', s), \quad (8)$$

where

$$\beta_l = \begin{cases} 0, & \langle \nabla_{\mathbf{E}} \mathcal{L}_B(\mathbf{X}', s), \nabla_{\mathbf{E}} \mathcal{L}_{\text{Attn}}(\mathbf{X}', p) \rangle > 0 \\ \frac{\langle \nabla_{\mathbf{E}} \mathcal{L}_S(\mathbf{X}', s), \nabla_{\mathbf{E}} \mathcal{L}_{\text{Attn}}(\mathbf{X}', p) \rangle}{\|\nabla_{\mathbf{E}} \mathcal{L}_S(\mathbf{X}', s)\|^2}, & \text{otherwise.} \end{cases} \quad (9)$$

Following PGD [37], we iteratively update \mathbf{E} using an Adam optimizer: $\mathbf{E}^{t+1} = \mathbf{E}^t + \eta \cdot \text{Adam}(\delta_{\mathbf{E}^t})$, where η is the step-size for each update.

4.3. Attention Weights Alignment

After Step 1, the DSA framework generates the adversarial example x' , whose top k patches containing spurious features are perturbed through the adversarial attack. Here, besides using these adversarial examples as augmentation during training of the debiased ViT model, we also leverage them via attention weights alignment to further guide the model to pay more attention to the real features. This further allows more spurious features to be discovered and ignored by the self-attention mechanism in the ViT model as shown in the right panel of Figure 2. In particular, we apply three different feature discrepancy metrics $D(\cdot, \cdot)$, i.e., Mean Squared Error (MSE), Kullback-Leibler Divergence

(KL-Div), and Attention Transfer (AT), to evaluate the discrepancy between the attention weights \mathbf{A}^x and $\mathbf{A}^{x'}$ from the original sample x and the adversarial example x' , respectively. We define the three metrics as:

$$D_{\text{MSE}}(\mathbf{A}^x, \mathbf{A}^{x'}) = \frac{1}{2} \sum_{j \in \mathcal{I}} \|\mathbf{A}_j^x - \mathbf{A}_j^{x'}\|_2, \quad (10)$$

$$D_{\text{KL-Div}}(\mathbf{A}^x, \mathbf{A}^{x'}) = \sum_{j \in \mathcal{I}} \mathbf{A}_j^x \log \frac{\mathbf{A}_j^x}{\mathbf{A}_j^{x'}}, \quad (11)$$

$$D_{\text{AT}}(\mathbf{A}^x, \mathbf{A}^{x'}) = \frac{1}{2} \sum_{j \in \mathcal{I}} \left\| \frac{\mathbf{A}_j^x}{\|\mathbf{A}_j^x\|_2} - \frac{\mathbf{A}_j^{x'}}{\|\mathbf{A}_j^{x'}\|_2} \right\|_2, \quad (12)$$

where \mathcal{I} denotes the indices of all the adversarial examples and the original example attention weights pairs for which we perform the alignment. Finally, to incorporate the attention distributions of \mathbf{A}^x and $\mathbf{A}^{x'}$ in the objective, we add $\mathcal{L}_A = D_*(\mathbf{A}^x, \mathbf{A}^{x'})$ as a regularizer in the overall training objective.

4.4. Overall Training Objective

Putting the above Steps 1 and 2 together, the overall objective for training the proposed debiased model is:

$$\mathcal{L} = \lambda_1 \mathcal{L}_{CE}(x, y) + \lambda_2 \mathcal{L}_{CE}(x', y) + \lambda_3 \mathcal{L}_A, \quad (13)$$

where \mathcal{L}_{CE} denotes the standard Cross-Entropy loss. λ_1, λ_2 , and λ_3 are three weighted coefficients for controlling the fairness-utility trade-off.

5. Experimental Settings

5.1. Datasets

We evaluate the DSA framework on three CV datasets widely used in the fairness research community, namely, Waterbirds [49], CelebA [31], and bFFHQ [25]. Waterbirds dataset contains spurious correlation between the background features $\mathcal{S} = \{\text{Water}, \text{Land}\}$ and target label $\mathcal{Y} = \{\text{Waterbird}, \text{Landbird}\}$. The spurious correlation is injected by pairing waterbirds with the water background and land birds with the land background more frequently, as compared to other combinations. CelebA dataset contains 200k celebrity face images with annotations for 40 binary attributes. We present the results on the settings following [56], where Hair Color (gray or not gray) is the target label the model is trained to predict and Gender is the sensitive label over which we wish the model to be unbiased. bFFHQ dataset has Age as a target label and Gender as a correlated bias. The images in the bFFHQ dataset include the dominant number of young women (i.e., aged 10-29) and old men (i.e., aged 40-59) in the training data. We provide more details of these datasets in Appendix.

Table 1: Fairness and accuracy evaluation for our methods, i.e., **DSA** together with in-house baseline **AM**, as well as other published baseline methods over different combinations of the target label (y) and the sensitive label (s) on the three datasets. For DSA, we use $\mathcal{L}_A = D_{AT}$ as the attention weight alignment regularizer. The test accuracies of the bias-only model used in DSA and the success rates of adversarial attacks are reported in Appendix. The best results are bold-faced.

Methods	Waterbirds Y: Bird Type S: Background					bFFHQ Y: Age S: Gender					CelebA Y: Hair Color S: Gender				
	EO↓	DP↓	DBA↓	BA(%)↑	Acc(%)↑	EO↓	DP↓	DBA↓	BA(%)↑	Acc(%)↑	EO↓	DP↓	DBA↓	BA(%)↑	Acc(%)↑
Vanilla	0.0209	0.0211	0.0841	60.24	62.36	0.3214	0.3410	0.1021	68.64	75.93	0.2763	0.3185	0.0422	81.84	90.25
TADeT	0.0424	0.0266	0.0747	64.14	69.05	0.3189	0.3318	0.0944	69.06	77.05	0.2850	0.2422	0.0427	81.27	90.23
MMD	0.0617	0.0380	0.0767	63.52	67.81	0.3041	0.2774	0.0847	70.59	76.59	0.3135	0.3023	0.0112	80.77	90.02
MFD	0.0386	0.0297	0.0736	63.01	67.36	0.2922	0.3135	0.0912	68.97	77.63	0.2812	0.3049	0.0237	81.74	90.41
DANN	0.0337	0.0238	0.0951	58.64	60.04	0.3067	0.3274	0.1141	69.87	76.75	0.2720	0.2586	0.0134	82.15	90.69
LAFTRE	0.0822	0.0415	0.0814	61.36	64.80	0.2936	0.3075	0.0961	70.05	76.67	0.3094	0.2682	0.0411	79.87	89.32
AM	0.0447	0.0332	0.0872	59.98	61.70	0.2874	0.2978	0.1021	70.91	78.76	0.2877	0.2621	0.0256	81.51	90.35
DSA	0.0185	0.0113	0.0709	63.87	69.58	0.2651	0.2856	0.0879	71.37	78.82	0.2558	0.2337	0.0031	82.92	90.95

5.2. Implementation Details

We train the ViT-S/16 models from scratch for each prediction task. The ViT-S/16 model consists of 196 patches (each representing a 16x16 sub-image), 1 class token patch, 12 transformer encoder layers, and 8 attention heads. We flatten and project each patch into a 64-dimensional vector and add positional embeddings. The embedded patches are fed into the ViT encoder. After the ViT encoder processes the patch embeddings, the class token patch is fed into 2 fully-connected layers (with a hidden state size of 256) and a sigmoid layer to produce a single normalized output score (since we deal with binary classification). We train the ViT models using momentum Stochastic Gradient Descent (SGD) with a momentum parameter of 0.9 and an initial learning rate of 3e-2 for 20 epochs. We use a fixed batch size of 32, gradient clipping at global norm 1, and a cosine decay learning rate schedule with a linear warmup following [16]. We select the model with the best accuracy on the validation sets.

5.3. Baselines

We select the following debiasing algorithms as baselines for performance evaluation, for which we select the best model that yields the highest validation performance. To our knowledge, besides the proposed DSA and the in-house baseline AM methods, TADeT is the only third-party fairness-aware algorithm tailor-made for ViT while all the others are designed for CNN. We consider the following baselines: **Vanilla** [11]: The ViT models are only trained with CE loss for target prediction. Mitigating Bias in ViT via Target Alignment (**TADeT**) [56] uses a targeted alignment strategy for debiasing ViT that aims to identify and remove bias primarily from query matrix features. Maximum Mean Discrepancy (**MMD**) [34] calculates the mean of penultimate layer feature activation values for each sensitive label setting and then minimizes their L_2 distance. MMD-based Fair Distillation (**MFD**) [23] adds an MMD-based regularizer that utilizes the group-indistinguishable predictive features from the teacher model while discouraging the

student model from discriminating against any protected group. Domain Adversarial Neural Network (**DANN**) [14] employs a sensitive label adversary learned on top of the penultimate layer activation. The adversarial head consists of two linear layers in the same dimension as the class token, followed by a sigmoid function. Learning Adversarially Fair and Transferable Representation (**LAFTRE**) [36] trains a model with a modified adversarial objective that attempts to meet the *EO* fairness criterion. This objective is implemented by minimizing the average absolute difference on each task. Attention Masking (**AM**): The self-attention mechanism is critical in ViT as it provides important weights for extracting visual features. We propose the AM method as a *home run* that directly masks the top- k patches with the highest attention scores for the bias-only model.

6. Results and Discussion

In this Section, we report the results of fairness and accuracy evaluations, the ablation study, and the effects of model size and patch size. In Appendix, more experimental results are reported, including the impact of several tunable hyperparameters, results with different D_* in the regularizer \mathcal{L}_A , and some other qualitative evaluations.

6.1. Fairness and Accuracy Evaluations

We report the fairness and accuracy performance of the three datasets in Table 1. We make the following observations. First, DSA outperforms the baselines on most evaluation metrics significantly improving the ViT fairness with lower EO, DP, and DBA while maintaining higher accuracy in terms of BA and ACC. Second, several baseline methods (e.g., MMD, MFD, and DANN) that have shown strong performance with CNN models, do not even outperform the vanilla model on some fairness metrics (e.g., EO), particularly on the waterbird dataset. This may happen because ViT primarily learns global image features by modeling long-range dependencies using the self-attention mechanism, which is fundamentally different from convolution-

Table 2: Ablation study of the three training objectives. The best results are bold-faced. ‘w/o’ represents without.

Models	Y: Hair Color S: Gender				
	EO↓	DP↓	DBA↓	BA↑	ACC↑
$\mathcal{L}(\text{all})$	0.2558	0.2337	0.0031	82.92	90.95
w/o $\mathcal{L}_{CE}(x, y)$	0.2754	0.2541	0.0175	81.21	88.32
w/o $\mathcal{L}_{CE}(x', y)$	0.2641	0.2503	0.0129	80.65	88.54
w/o \mathcal{L}_A	0.2934	0.2865	0.0206	81.54	89.91

based local feature learning with CNN. As such, these baseline methods (designed for the CNNs) are not transferable for bias mitigation with the ViT models. Third, we note the in-house baseline method AM is also designed by blinding the spurious features in the input based on only the attention weights of the bias-only model. However, several works [52, 22, 1] have questioned whether highly attentive inputs would significantly impact the model outputs. Since the self-attention mechanism involves the computation of queries, keys, and values, reducing it only to the derived attention weights (inner products of queries and keys) can be insufficient to capture the importance of the features. Hence, the *home run* AM method fails to achieve comparable performance with the proposed DSA method.

6.2. Ablating DSA

The objective of DSA contains three components for bias mitigation as shown in Eq.13. We conduct an ablation study on the CelebA dataset to analyze their individual contributions and report the results in Table 2. We summarize our major findings. First, all of the components contribute towards improved fairness performance across all three fairness metrics. Second, both the target CE losses in Eq.(13) are critical in preventing DSA from compromising the prediction performance (otherwise, the accuracy drops from 90.95 to 88.32 and 88.54, respectively). Third, the regularizer \mathcal{L}_A contributes the most to the higher fairness measures, as is clearly shown by: EO (0.2934→0.2558), DP (0.2865→0.2337), and DBA (0.0206→0.0031).

6.3. Effect of ViT Model Size and Patch Size

We examine the effect of ViT model size and patch size on DSA in Table 3. The ViT-B model is much larger than the ViT-S model, which has 12 self-attention heads in each block and 256 hidden state sizes in the two fully-connected layers. Each patch is flattened and projected into a vector of 768 dimensions. We draw two conclusions from Table 3. First, the larger ViT-B models outperform the smaller ViT-S on most of the fairness and accuracy metrics, demonstrating better feature learning capabilities with higher feature dimensions and more self-attention heads. Second, a smaller patch size (16) achieves a better performance on both fairness and accuracy measurements because small patches enable extracting more fine-grained features [5].

Table 3: Performance evaluation with different ViT models (i.e., ViT-B (B) and ViT-S (S)) and patch sizes (i.e., 16 and 32). All tunable hyper-parameters are set to the same as in Table 1. VA denotes the vanilla ViT.

Model		Y: Hair Color S: Gender				
		EO↓	DP↓	DBA↓	BA↑	ACC↑
B/16	VA	0.2984	0.2841	0.0142	81.95	91.05
	DSA	0.2424	0.2205	0.0081	83.42	91.24
S/16	VA	0.2763	0.3185	0.0422	81.84	90.25
	DSA	0.2558	0.2337	0.0031	82.92	90.95
B/32	VA	0.2982	0.2976	0.0205	81.11	90.16
	DSA	0.2629	0.2520	0.0109	82.73	91.03
S/32	VA	0.3014	0.3213	0.0198	80.64	89.18
	DSA	0.2935	0.3165	0.0086	80.86	89.45

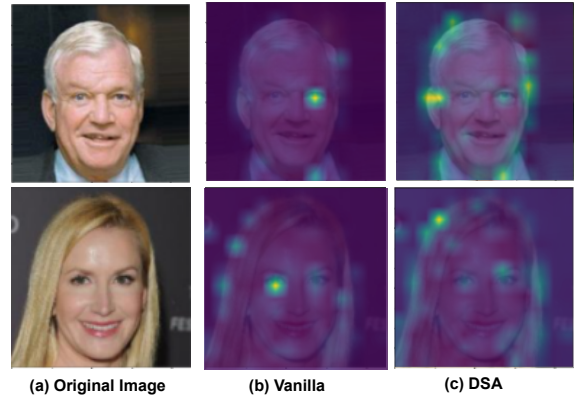


Figure 3: Qualitative evaluation. Y: Hair Color, S: Gender.

6.4. Qualitative Evaluations

The examples in Figures 3 further demonstrate the effectiveness of the DSA approach. We note that the distribution of the attention weights for the vanilla ViT model largely focuses on the spurious feature, e.g., ‘eye shadow’. This demonstrates that the vanilla ViT model simply leverages the spurious features to predict the target label. On the contrary, DSA reduces the attention to these spurious features but pays more attention to the real features, e.g., ‘hair’.

7. Conclusion

In this work, we proposed a novel hierarchical fairness-aware ViT training framework named DSA for bias mitigation in both the training set and the learning algorithm while maintaining prediction performance. DSA is designed to eliminate spurious features in the data through adversarial attacks on the bias-only model, while also retaining the informative features through an attention weights alignment regularizer. The quantitative and qualitative experimental results demonstrate the effectiveness of DSA for bias mitigation without compromising prediction performance.

References

- [1] Samira Abnar and Willem Zuidema. Quantifying attention flow in transformers. *arXiv preprint arXiv:2005.00928*, 2020.
- [2] Srinadh Bhojanapalli, Ayan Chakrabarti, Daniel Glasner, Daliang Li, Thomas Unterthiner, and Andreas Veit. Understanding robustness of transformers for image classification. In *Proceedings of the IEEE/CVF International Conference on Computer Vision*, pages 10231–10241, 2021.
- [3] Nicolas Carion, Francisco Massa, Gabriel Synnaeve, Nicolas Usunier, Alexander Kirillov, and Sergey Zagoruyko. End-to-end object detection with transformers. In *European conference on computer vision*, pages 213–229. Springer, 2020.
- [4] Hila Chefer, Shir Gur, and Lior Wolf. Transformer interpretability beyond attention visualization. In *Proceedings of the IEEE/CVF Conference on Computer Vision and Pattern Recognition*, pages 782–791, 2021.
- [5] Chun-Fu Richard Chen, Quanfu Fan, and Rameswar Panda. Crossvit: Cross-attention multi-scale vision transformer for image classification. In *Proceedings of the IEEE/CVF international conference on computer vision*, pages 357–366, 2021.
- [6] Minghao Chen, Houwen Peng, Jianlong Fu, and Haibin Ling. Autoformer: Searching transformers for visual recognition. In *Proceedings of the IEEE/CVF International Conference on Computer Vision*, pages 12270–12280, 2021.
- [7] Alexandra Chouldechova and Aaron Roth. The frontiers of fairness in machine learning. *arXiv preprint arXiv:1810.08810*, 2018.
- [8] Ching-Yao Chuang and Youssef Mroueh. Fair mixup: Fairness via interpolation. *arXiv preprint arXiv:2103.06503*, 2021.
- [9] Zhigang Dai, Bolun Cai, Yugeng Lin, and Junying Chen. Up-detr: Unsupervised pre-training for object detection with transformers. In *Proceedings of the IEEE/CVF conference on computer vision and pattern recognition*, pages 1601–1610, 2021.
- [10] Jacob Devlin, Ming-Wei Chang, Kenton Lee, and Kristina Toutanova. Bert: Pre-training of deep bidirectional transformers for language understanding. *arXiv preprint arXiv:1810.04805*, 2018.
- [11] Alexey Dosovitskiy, Lucas Beyer, Alexander Kolesnikov, Dirk Weissenborn, Xiaohua Zhai, Thomas Unterthiner, Mostafa Dehghani, Matthias Minderer, Georg Heigold, Sylvain Gelly, et al. An image is worth 16x16 words: Transformers for image recognition at scale. *arXiv preprint arXiv:2010.11929*, 2020.
- [12] Cynthia Dwork, Moritz Hardt, Toniann Pitassi, Omer Reingold, and Richard Zemel. Fairness through awareness. In *Proceedings of the 3rd innovations in theoretical computer science conference*, pages 214–226, 2012.
- [13] Yonggan Fu, Shun Yao Zhang, Shang Wu, Cheng Wan, and Yingyan Lin. Patch-fool: Are vision transformers always robust against adversarial perturbations? *arXiv preprint arXiv:2203.08392*, 2022.
- [14] Yaroslav Ganin and Victor Lempitsky. Unsupervised domain adaptation by backpropagation. In *International conference on machine learning*, pages 1180–1189. PMLR, 2015.
- [15] Robert Geirhos, Jörn-Henrik Jacobsen, Claudio Michaelis, Richard Zemel, Wieland Brendel, Matthias Bethge, and Felix A Wichmann. Shortcut learning in deep neural networks. *Nature Machine Intelligence*, 2(11):665–673, 2020.
- [16] Soumya Suvra Ghosal, Yifei Ming, and Yixuan Li. Are vision transformers robust to spurious correlations? *arXiv preprint arXiv:2203.09125*, 2022.
- [17] Jindong Gu, Volker Tresp, and Yao Qin. Are vision transformers robust to patch perturbations? In *European Conference on Computer Vision*, pages 404–421. Springer, 2022.
- [18] Moritz Hardt, Eric Price, and Nati Srebro. Equality of opportunity in supervised learning. *Advances in neural information processing systems*, 29, 2016.
- [19] Kaiming He, Xiangyu Zhang, Shaoqing Ren, and Jian Sun. Deep residual learning for image recognition. In *Proceedings of the IEEE conference on computer vision and pattern recognition*, pages 770–778, 2016.
- [20] Kenneth Holstein, Jennifer Wortman Vaughan, Hal Daumé III, Miro Dudík, and Hanna Wallach. Improving fairness in machine learning systems: What do industry practitioners need? In *Proceedings of the 2019 CHI conference on human factors in computing systems*, pages 1–16, 2019.
- [21] Drew A Hudson and Larry Zitnick. Generative adversarial transformers. In *International conference on machine learning*, pages 4487–4499. PMLR, 2021.
- [22] Sarthak Jain and Byron C Wallace. Attention is not explanation. *arXiv preprint arXiv:1902.10186*, 2019.
- [23] Sangwon Jung, Donggyu Lee, Taeon Park, and Taesup Moon. Fair feature distillation for visual recognition. In *Proceedings of the IEEE/CVF conference on computer vision and pattern recognition*, pages 12115–12124, 2021.
- [24] Byungju Kim, Hyunwoo Kim, Kyungsu Kim, Sungjin Kim, and Junmo Kim. Learning not to learn: Training deep neural networks with biased data. In *Proceedings of the IEEE/CVF Conference on Computer Vision and Pattern Recognition*, pages 9012–9020, 2019.
- [25] Eungyeup Kim, Jihyeon Lee, and Jaegul Choo. Biaswap: Removing dataset bias with bias-tailored swapping augmentation. In *Proceedings of the IEEE/CVF International Conference on Computer Vision*, pages 14992–15001, 2021.
- [26] Michael P Kim, Amirata Ghorbani, and James Zou. Multi-accuracy: Black-box post-processing for fairness in classification. In *Proceedings of the 2019 AAAI/ACM Conference on AI, Ethics, and Society*, pages 247–254, 2019.
- [27] Xin Li, Xiangrui Li, Deng Pan, and Dongxiao Zhu. Improving adversarial robustness via probabilistically compact loss with logit constraints. In *Proceedings of the AAAI Conference on Artificial Intelligence*, volume 35, pages 8482–8490, 2021.
- [28] Yawei Li, Kai Zhang, Jie Zhang Cao, Radu Timofte, and Luc Van Gool. Localvit: Bringing locality to vision transformers. *arXiv preprint arXiv:2104.05707*, 2021.

- [29] Zhiheng Li, Anthony Hoogs, and Chenliang Xu. Discover and mitigate unknown biases with debiasing alternate networks. In *European Conference on Computer Vision*, pages 270–288. Springer, 2022.
- [30] Ze Liu, Yutong Lin, Yue Cao, Han Hu, Yixuan Wei, Zheng Zhang, Stephen Lin, and Baining Guo. Swin transformer: Hierarchical vision transformer using shifted windows. In *Proceedings of the IEEE/CVF International Conference on Computer Vision*, pages 10012–10022, 2021.
- [31] Ziwei Liu, Ping Luo, Xiaogang Wang, and Xiaoou Tang. Deep learning face attributes in the wild. In *Proceedings of the IEEE international conference on computer vision*, pages 3730–3738, 2015.
- [32] Francesco Locatello, Gabriele Abbati, Thomas Rainforth, Stefan Bauer, Bernhard Schölkopf, and Olivier Bachem. On the fairness of disentangled representations. *Advances in Neural Information Processing Systems*, 32, 2019.
- [33] Pranay K Lohia, Karthikeyan Natesan Ramamurthy, Manish Bhide, Diptikalyan Saha, Kush R Varshney, and Ruchir Puri. Bias mitigation post-processing for individual and group fairness. In *Icassp 2019-2019 IEEE international conference on acoustics, speech and signal processing (icassp)*, pages 2847–2851. IEEE, 2019.
- [34] Mingsheng Long, Yue Cao, Jianmin Wang, and Michael Jordan. Learning transferable features with deep adaptation networks. In *International conference on machine learning*, pages 97–105. PMLR, 2015.
- [35] Andreas Lugmayr, Martin Danelljan, Andres Romero, Fisher Yu, Radu Timofte, and Luc Van Gool. Repaint: Inpainting using denoising diffusion probabilistic models. In *Proceedings of the IEEE/CVF Conference on Computer Vision and Pattern Recognition (CVPR)*, pages 11461–11471, June 2022.
- [36] David Madras, Elliot Creager, Toniann Pitassi, and Richard Zemel. Learning adversarially fair and transferable representations. In *International Conference on Machine Learning*, pages 3384–3393. PMLR, 2018.
- [37] Aleksander Madry, Aleksandar Makelov, Ludwig Schmidt, Dimitris Tsipras, and Adrian Vladu. Towards deep learning models resistant to adversarial attacks. *arXiv preprint arXiv:1706.06083*, 2017.
- [38] Xiaofeng Mao, Gege Qi, Yuefeng Chen, Xiaodan Li, Ranjie Duan, Shaokai Ye, Yuan He, and Hui Xue. Towards robust vision transformer. In *Proceedings of the IEEE/CVF Conference on Computer Vision and Pattern Recognition*, pages 12042–12051, 2022.
- [39] Tyler McDonnell, Matthew Lease, Mucahid Kutlu, and Tamer Elsayed. Why is that relevant? collecting annotator rationales for relevance judgments. In *Proceedings of the AAAI Conference on Human Computation and Crowdsourcing*, volume 4, pages 139–148, 2016.
- [40] Junhyun Nam, Hyuntak Cha, Sungsoo Ahn, Jaeho Lee, and Jinwoo Shin. Learning from failure: De-biasing classifier from biased classifier. *Advances in Neural Information Processing Systems*, 33:20673–20684, 2020.
- [41] Muzammal Naseer, Kanchana Ranasinghe, Salman Khan, Fahad Shahbaz Khan, and Fatih Porikli. On improving adversarial transferability of vision transformers. *arXiv preprint arXiv:2106.04169*, 2021.
- [42] Deng Pan, Xin Li, and Dongxiao Zhu. Explaining deep neural network models with adversarial gradient integration. In *IJCAI*, pages 2876–2883, 2021.
- [43] Sungho Park, Dohyung Kim, Sunhee Hwang, and Hyeran Byun. Readme: Representation learning by fairness-aware disentangling method. *arXiv preprint arXiv:2007.03775*, 2020.
- [44] Sayak Paul and Pin-Yu Chen. Vision transformers are robust learners. In *Proceedings of the AAAI Conference on Artificial Intelligence*, volume 36, pages 2071–2081, 2022.
- [45] Francesco Pinto, Philip Torr, and Puneet K Dokania. Are vision transformers always more robust than convolutional neural networks? 2021.
- [46] Yao Qiang, Chengyin Li, Marco Brocanelli, and Dongxiao Zhu. Counterfactual interpolation augmentation (cia): A unified approach to enhance fairness and explainability of dnn. In *Proceedings of the Thirty-First International Joint Conference on Artificial Intelligence, IJCAI-22, LD Raedt, Ed. International Joint Conferences on Artificial Intelligence Organization*, volume 7, pages 732–739, 2022.
- [47] Yao Qiang, Deng Pan, Chengyin Li, Xin Li, Rhongho Jang, and Dongxiao Zhu. AttCAT: Explaining transformers via attentive class activation tokens. In Alice H. Oh, Alekh Agarwal, Danielle Belgrave, and Kyunghyun Cho, editors, *Advances in Neural Information Processing Systems*, 2022.
- [48] Prajit Ramachandran, Niki Parmar, Ashish Vaswani, Irwan Bello, Anselm Levskaya, and Jon Shlens. Stand-alone self-attention in vision models. *Advances in Neural Information Processing Systems*, 32, 2019.
- [49] Shiori Sagawa, Pang Wei Koh, Tatsunori B Hashimoto, and Percy Liang. Distributionally robust neural networks for group shifts: On the importance of regularization for worst-case generalization. *arXiv preprint arXiv:1911.08731*, 2019.
- [50] Hadi Salman, Saachi Jain, Eric Wong, and Aleksander Madry. Certified patch robustness via smoothed vision transformers. In *Proceedings of the IEEE/CVF Conference on Computer Vision and Pattern Recognition*, pages 15137–15147, 2022.
- [51] Mhd Hasan Sarhan, Nassir Navab, Abouzar Eslami, and Shadi Albarqouni. Fairness by learning orthogonal disentangled representations. In *European Conference on Computer Vision*, pages 746–761. Springer, 2020.
- [52] Sofia Serrano and Noah A Smith. Is attention interpretable? *arXiv preprint arXiv:1906.03731*, 2019.
- [53] Rulin Shao, Zhouxing Shi, Jinfeng Yi, Pin-Yu Chen, and Cho-Jui Hsieh. On the adversarial robustness of vision transformers. *arXiv preprint arXiv:2103.15670*, 2021.
- [54] Krishna Kumar Singh, Dhruv Mahajan, Kristen Grauman, Yong Jae Lee, Matt Feiszli, and Deepti Ghadiyaram. Don’t judge an object by its context: learning to overcome contextual bias. In *Proceedings of the IEEE/CVF Conference on Computer Vision and Pattern Recognition*, pages 11070–11078, 2020.
- [55] Robin Strudel, Ricardo Garcia, Ivan Laptev, and Cordelia Schmid. Segmenter: Transformer for semantic segmenta-

- tion. In *Proceedings of the IEEE/CVF International Conference on Computer Vision*, pages 7262–7272, 2021.
- [56] Sruthi Sudhakar, Viraj Prabhu, Arvindkumar Krishnakumar, and Judy Hoffman. Mitigating bias in visual transformers via targeted alignment. 2021.
- [57] Ashish Vaswani, Noam Shazeer, Niki Parmar, Jakob Uszkoreit, Llion Jones, Aidan N Gomez, Łukasz Kaiser, and Illia Polosukhin. Attention is all you need. *Advances in neural information processing systems*, 30, 2017.
- [58] Mei Wang and Weihong Deng. Mitigating bias in face recognition using skewness-aware reinforcement learning. In *Proceedings of the IEEE/CVF conference on computer vision and pattern recognition*, pages 9322–9331, 2020.
- [59] Wentao Wang, Li Niu, Jianfu Zhang, Xue Yang, and Liqing Zhang. Dual-path image inpainting with auxiliary gan inversion. In *Proceedings of the IEEE/CVF Conference on Computer Vision and Pattern Recognition*, pages 11421–11430, 2022.
- [60] Zhibo Wang, Xiaowei Dong, Henry Xue, Zhifei Zhang, Weifeng Chiu, Tao Wei, and Kui Ren. Fairness-aware adversarial perturbation towards bias mitigation for deployed deep models. In *Proceedings of the IEEE/CVF Conference on Computer Vision and Pattern Recognition*, pages 10379–10388, 2022.
- [61] Benjamin Wilson, Judy Hoffman, and Jamie Morgenstern. Predictive inequity in object detection. *arXiv preprint arXiv:1902.11097*, 2019.
- [62] Han Xu, Xiaorui Liu, Yaxin Li, Anil Jain, and Jiliang Tang. To be robust or to be fair: Towards fairness in adversarial training. In *International Conference on Machine Learning*, pages 11492–11501. PMLR, 2021.
- [63] Jianwei Yang, Chunyuan Li, Pengchuan Zhang, Xiyang Dai, Bin Xiao, Lu Yuan, and Jianfeng Gao. Focal self-attention for local-global interactions in vision transformers. *arXiv preprint arXiv:2107.00641*, 2021.
- [64] Tianhe Yu, Saurabh Kumar, Abhishek Gupta, Sergey Levine, Karol Hausman, and Chelsea Finn. Gradient surgery for multi-task learning. *Advances in Neural Information Processing Systems*, 33:5824–5836, 2020.
- [65] Brian Hu Zhang, Blake Lemoine, and Margaret Mitchell. Mitigating unwanted biases with adversarial learning. In *Proceedings of the 2018 AAAI/ACM Conference on AI, Ethics, and Society*, pages 335–340, 2018.
- [66] Yi Zhang and Jitao Sang. Towards accuracy-fairness paradox: Adversarial example-based data augmentation for visual debiasing. In *Proceedings of the 28th ACM International Conference on Multimedia*, pages 4346–4354, 2020.
- [67] Sixiao Zheng, Jiachen Lu, Hengshuang Zhao, Xiatian Zhu, Zekun Luo, Yabiao Wang, Yanwei Fu, Jianfeng Feng, Tao Xiang, Philip HS Torr, et al. Rethinking semantic segmentation from a sequence-to-sequence perspective with transformers. In *Proceedings of the IEEE/CVF conference on computer vision and pattern recognition*, pages 6881–6890, 2021.
- [68] Daquan Zhou, Zhiding Yu, Enze Xie, Chaowei Xiao, Animeshree Anandkumar, Jiashi Feng, and Jose M Alvarez. Understanding the robustness in vision transformers. In *International Conference on Machine Learning*, pages 27378–27394. PMLR, 2022.

8. Appendix

8.1. Dataset Statistics

We first provide the data statistics of three used datasets in Figure 4. We note that significant biases exist in these datasets. For example, a majority of “Gray Hair” are correlated with “Male” whereas the majority of “None Gray Hair” are correlated with “Female” in CelebA dataset. Similar spurious correlations are also observed in other datasets as well, which can lead to biased models.

8.2. Performance of Vanilla ViT

We further establish the bias issues by analyzing and reporting the True Positive Rate (TPR) of the vanilla ViT models trained on these datasets in Table 4. Clearly, the biased ViT models perform significantly worse on the minority groups, e.g., predicting “gray hair” when the individual is female ($S = 0$: 63.31%) compared to the ones that are male ($S = 1$: 95.16%).

Table 4: TPR and disparities of TPR among different target and sensitive attribute tuples.

Datasets	Y	S	TPR% \uparrow	Δ TPR%
bFFHQ	Age	Female (0)	64.93	23.57
		Male (1)	88.50	
CelebA	Hair Color	Female (0)	63.31	31.85
		Male (1)	95.16	
Waterbird	Waterbird	Land (0)	55.75	14.14
		Water (1)	69.89	

8.3. Effect of Discrepancy Metrics

Since three different metrics $D(\cdot, \cdot)$, i.e., MSE, KL-Div, and AT, are applied to evaluate the discrepancy between the attention weights \mathbf{A}^x and $\mathbf{A}^{x'}$ in Eq. (13), we report the effect of these discrepancy metrics in Table 5. Although the differences between these discrepancy metrics are relatively small, AT clearly achieves the best performance, especially on the fairness metrics, i.e, EO, DP, and DBA. Since AT can capture the most significant differences between \mathbf{A}^x and $\mathbf{A}^{x'}$ as shown in Eq. (12), the regularizer \mathcal{L}_A is more efficient to minimize their differences.

Table 5: Evaluations with different discrepancy metrics in the regularizer of the final objective function Eq. (13) on CelebA dataset.

D_*	Y: Hair Color S: Gender				
	EO \downarrow	DP \downarrow	DBA \downarrow	BA \uparrow	Acc% \uparrow
MSE	0.2706	0.2488	0.0136	82.07	90.13
KL-Div	0.2608	0.2467	0.0106	83.26	89.48
AT	0.2558	0.2337	0.0031	82.92	90.95

8.4. Effect of Tunable Hyper-parameters

There are several tunable hyper-parameters in the proposed DSA framework, including the various coefficient weights in the objective function and the number of masked patches learned during the adversarial attack.

We tune the three coefficient weights in the objective function Eq. (13) to identify the best-performing model as shown in Table 6. To improve model performance, we believe that these coefficient weights should be carefully tuned and selected under different settings and datasets.

The effect of the number of masked patches learned during the adversarial attack is shown in Table 7. In our experiments, the ViT model with $k = 3$ patches achieves the best performance among all compared metrics in most settings. Looking into more details of the adversarial examples shown in Figure 5, if we perturb only one patch out of all the input patches, some sensitive attributes may not be localized and masked. On the contrary, perturbing excessive patches (e.g., 5 patches) would increase the risk of masking the related attributes to the target task, resulting in worse prediction performance. For example, the Acc drops from 90.95 to 88.55 in the setting of (Hair Color, Gender) with 5 perturbed patches, as shown in Table 7.

Table 6: Evaluations with different tunable coefficient weights in the objective function Eq.(13) on CelebA dataset.

$\lambda_1, \lambda_2, \lambda_3$	Y: Hair Color S: Gender				
	EO \downarrow	DP \downarrow	DBA \downarrow	BA \uparrow	Acc% \uparrow
1.0, 0.5, 0.5	0.2843	0.2675	0.0125	81.45	91.12
0.5, 1.0, 0.5	0.2633	0.2578	0.0106	81.32	89.26
1.0, 1.0, 0.5	0.2558	0.2337	0.0031	82.92	90.95

Table 7: Performance of DSA with the different number of perturbed patches (k) during the adversarial attack on CelebA dataset.

k	Y: Hair Color S: Gender				
	EO \downarrow	DP \downarrow	DBA \downarrow	BA(%) \uparrow	Acc(%) \uparrow
1	0.2946	0.3075	0.0110	81.77	90.61
3	0.2558	0.2337	0.0031	82.92	90.95
5	0.2776	0.2560	0.0216	81.91	88.55

8.5. Adversarial Attack and Examples

We show the adversarial attack success rates of DSA on three datasets in Table 8. As discussed before, although the more perturbed patches lead to higher adversarial attack success rates, it would also increase the risk of masking the related attributes to the target task, resulting in a worse prediction performance as shown in Table 7 and Figure 5.

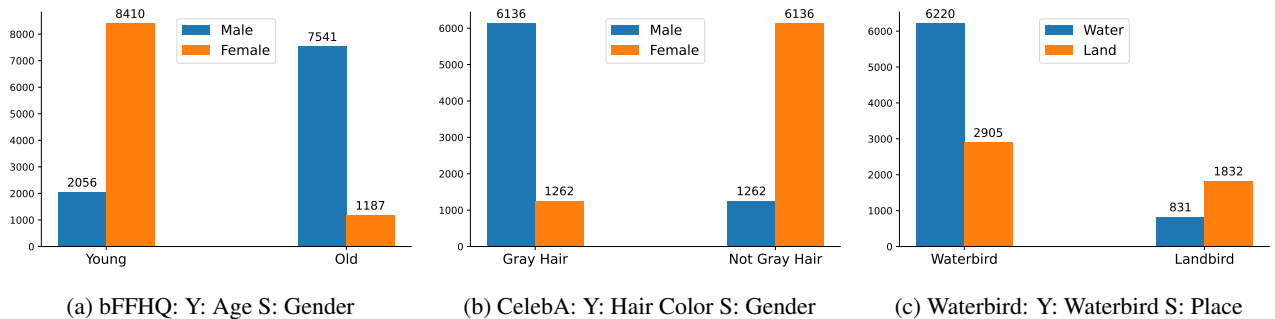


Figure 4: Spurious correlation between tasks (Y) and sensitive attributes (S) tuples (Y, S).

Table 8: Adversarial attack success rates of DSA on the sensitive attributes target with the different number of perturbed patches (k) on different datasets.

Datasets	S	k	Success Rate% \uparrow
bFFHQ	Gender	1	85.69
		3	88.73
		5	90.25
CelebA	Gender	1	88.52
		3	91.47
		5	93.69
Waterbird	Place	1	85.41
		3	90.11
		5	91.64

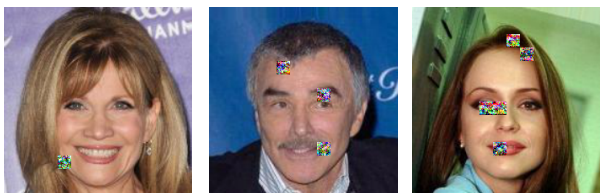


Figure 5: Adversarial examples with the different number of perturbed patches on CelebA dataset.